ACS NANO

www.acsnano.org

ARTICLE

Hydrogel Nanocomposites with Independently Tunable Rheology and Mechanics

Shimon Unterman,*[,†] Lyndon F. Charles,[†] Sara E. Strecker,[†] Denis Kramarenko,[†,‡] Dmitry Pivovarchik,[†,‡] Elazer R. Edelman,[†,§] and Natalie Artzi*[,†,⊥]

[†]Massachusetts Institute of Technology, Institute for Medical Engineering and Science, 45 Carleton Street, E25-438, Cambridge, Massachusetts 02139, United States

[‡]Ort Braude College, 51 Swallow Street, Karmiel, 2161002 Haifa, Israel

[§]Cardiovascular Division, Brigham and Women's Hospital, Harvard Medical School, Boston, Massachusetts 02115, United States

[⊥]Department of Medicine Division of Biomedical Engineering Brigham and Women's Hospital, Harvard Medical School, Boston, Massachusetts 02115, United States

Supporting Information

ABSTRACT: **Hydrogels are an attractive class of biomaterials for minimally invasive local drug delivery given their injectability, tunability, high water content, and biocompatibility. Broad applicability though is challenged: relatively modest mechanical properties restrict use to soft tissues, while flow properties necessary for injectability limit implantation to dried, enclosed tissues to minimize material migration during gelation. To address these dual concerns, we designed an injectable nanocomposite hydrogel based on dextran aldehyde and a poly(amido amine) dendrimer doped with phyllosilicate nanoplatelet fillers. Balance of components allows for exfoliation of nanoplatelets, significantly changing macromer solution flow, facilitating injection and manipulation in a wide variety of implantation contexts while enhancing compressive modulus of hydrogels at low loading. Importantly, rheological and mechanical effects were dependent on aspect ratio, with high aspect ratio nanoplatelets having much stronger effects on mechanics and low aspect ratio nanoplatelets having stronger effects on rheology, enabling nearly independent control of rheological and mechanical properties. Nanoplatelets enhanced hydrogel properties at a filler loading substantially lower than that of comparably sized nanoparticles. We present a model to explain the role that aspect ratio plays in control of rheology and mechanics in nanoplatelet-containing hydrogels, with lessons for further nanocomposite hydrogel development. This low-cost biocompatible material may be useful as a drug delivery platform in challenging implantation environments.**

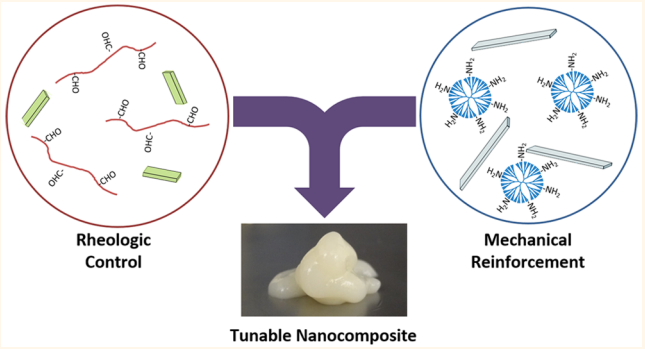

KEYWORDS: *nanocomposite, hydrogel, nanoplatelet, phyllosilicate, rheology, mechanics, aspect ratio*

Hydrogels are a widely used class of polymeric biomaterial characterized by high water content and excellent biocompatibility. They are attractive for applications in drug delivery and tissue engineering given the rapid diffusion of nutrients or drugs through the material, facile modification with a variety of chemical and biological functionalities, and easy encapsulation of cells and drugs. Hydrogels have been proposed for use as tissue sealants, local delivery of drugs and genes, and cell delivery.[1−5] Importantly, many hydrogels can be implanted in a minimally invasive manner by injection, forming a gel *in situ*. Injectable hydrogels typically are cross-linked using photo-cross-linking, spontaneous reactions upon mixing of two or more solutions, or self-assembly. Injectability substantially expands their potential clinical utility while reducing the morbidity encountered with more invasive implantation routes.[6−8]

However, hydrogels often exhibit poor rheological and mechanical properties that limit their usefulness in challenging implantation environments. Injectability necessitates macromer solutions with relatively low viscosity to allow for unimpeded flow during injection. These flow properties are incompatible with many implantation sites that are in inverted or poorly contained geometries; other sites, such as in arthroscopic surgeries, are also submerged or washed with saline that rapidly

Received: October 6, 2016
Accepted: February 21, 2017
Published: February 21, 2017

DOI: 10.1021/acsnano.6b06730
ACS Nano 2017, 11, 2598−2610

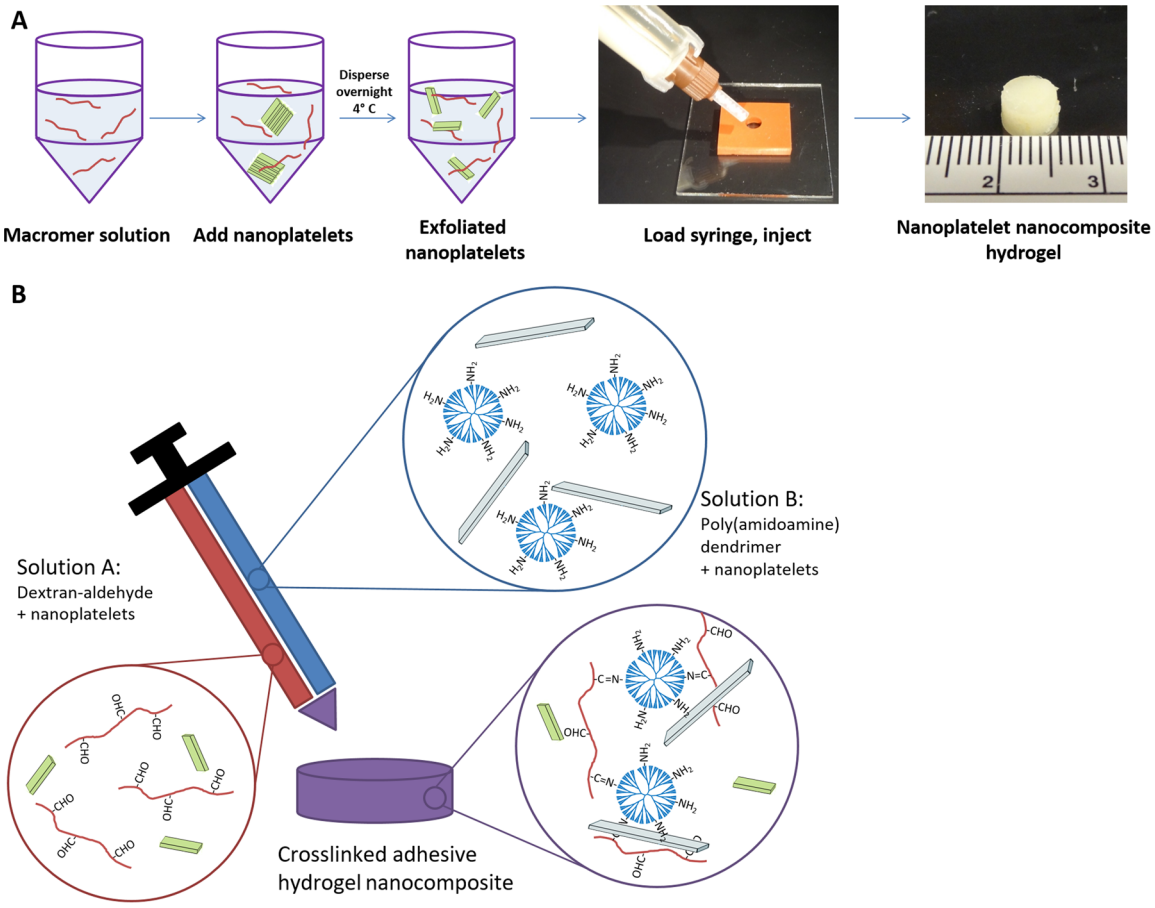

Figure 1. Preparation of nanoplatelet nanocomposite hydrogels. (A) Tactoids of stacked nanoplatelets are added directly to aqueous macromer solutions and dispersed overnight. Each nanofiller-containing macromer solution is then loaded into a two-barrelled syringe and injected into a mold for polymerization, yielding a hydrogel within minutes (cm scale ruler). (B) Hydrogels are mixed from dextran−aldehyde and PAMAM dendrimer−amine solutions, each potentially containing a nanofiller. The aldehydes and amines spontaneously react upon mixing to form a Schiff base.

dilutes injected solutions. Furthermore, injectable hydrogels typically exhibit poor mechanical properties, with elastic moduli in the tens of kPa or lower.[9,10] Attempts to increase cross-linking can partially ameliorate this concern but at the cost of decreased surgical working time and increased brittleness. Thus, a substantial need exists for hydrogels that exhibit excellent control over rheological and mechanical properties without sacrificing injectability or other desired properties stemming from their high water content.

Several approaches have been proposed to address this need, frequently including multiple gelation methodologies used in tandem: a weak, reversible, fast-acting cross-linking for immediate shape retention and resistance to flow coupled with a stronger, permanent, slower-acting cross-linking for enhanced material stability. Previous studies have exploited lower critical solution temperature (LCST) behavior, self-assembly, ionic cross-linking, and supramolecular assembly to provide for rapid onset gelation.[11−18] While elegant and promising, these approaches typically require a limited selection of polymers specifically designed to impart these behaviors, which may impede the optimization of hydrogels for other functions.

In contrast, others have doped unmodified polymer designs with fillers to create composites with modified rheological and mechanical properties. Of particular interest are nanocomposites, which incorporate nanoscale fillers into the hydrogel. These nanofillers interact with the surrounding polymer phase to alter rheological properties of macromer solutions and increase stiffness of cross-linked hydrogels.[19−22] However, there is little systematic research into the role of particle size, shape, and composition in tuning rheological and mechanical properties of injectable hydrogels. Furthermore, while some proposed formulations appropriately tune rheological *or* mechanical properties, they struggle to tune both properties independently; also, other nanocomposites require relatively high nanofiller loading to appreciably affect material properties, compromising other desired properties.

In addition to particulate and fibrous nanofillers, increasing interest has focused on the use of platelet-shaped nanofillers for use in nanocomposite materials.[19,23−26] These nanoplatelets typically have thicknesses on the order of 1 nm or less but lateral dimensions ranging from 20 nm to as much as 1 μm. They exhibit extraordinarily high surface area per unit of mass, allowing for high levels of interaction with adjacent nanoplatelets and with the polymer phase. Nanoplatelets, particular phyllosilicates, have a long history in industrial applications to strengthen hydrophobic polymers such as nylon-6 and rubber.[27] Separately, nanoplatelets have been used as rheological modifiers in drilling mud, asphalt, cosmetics, and other applications.[28−31] In recent years, there has been greater interest in extending nanoplatelet composites to hydrophilic polymer systems such as poly(vinyl alcohol) and *N*-isopropyl-

DOI: 10.1021/acsnano.6b06730
ACS Nano 2017, 11, 2598−2610

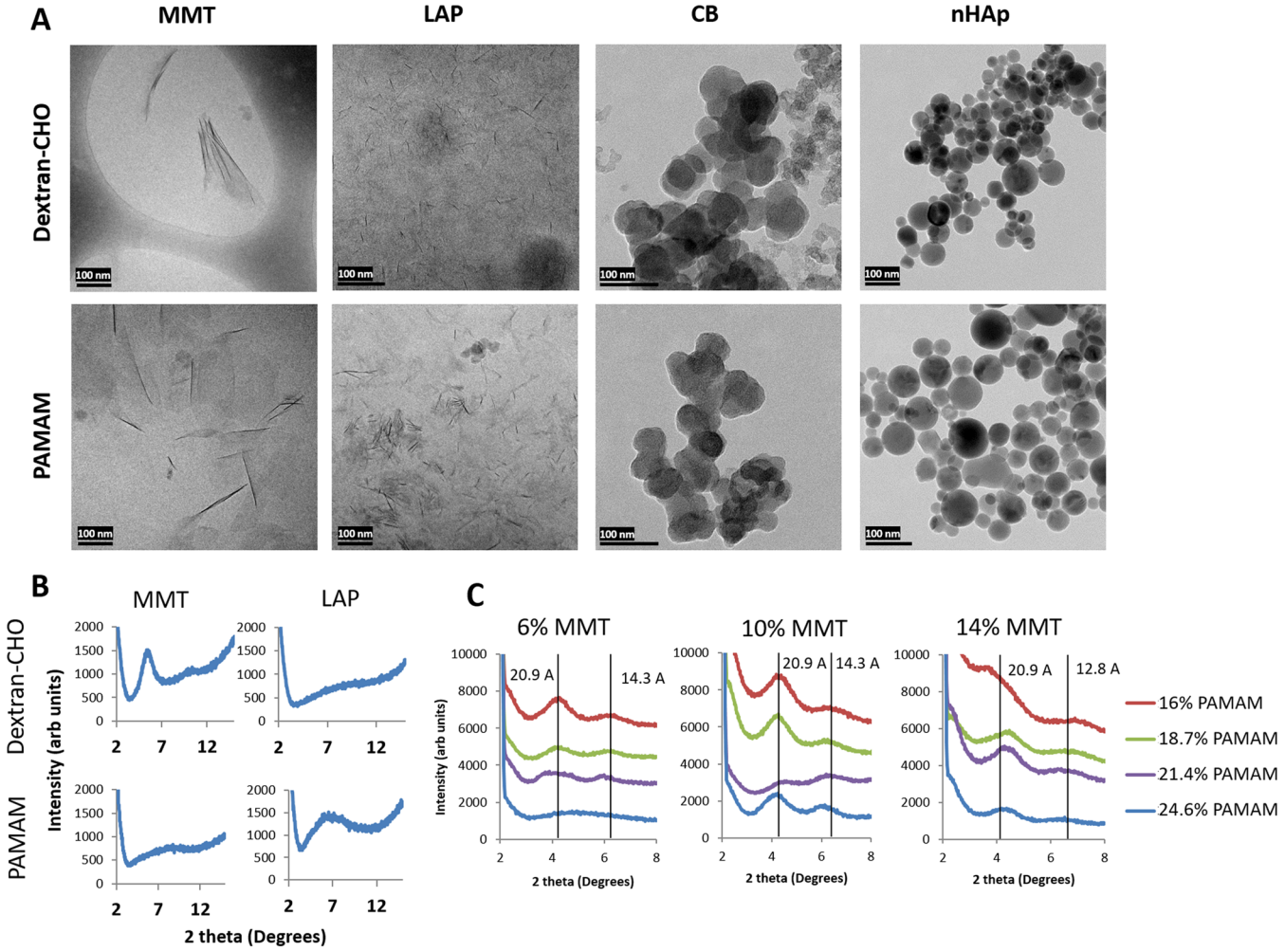

Figure 2. Morphology and dispersion of nanofillers. (A) Cryo-TEM of dispersions of each of four nanofillers in either 20% dextran−aldehyde or 24.6% PAMAM dendrimer macromer solutions. MMT = montmorillonite, 6%; LAP = Laponite, 6%; CB = carbon black, 5%; nHAp = nanoscale hydroxyapatite, 5%. Every dispersion was diluted 1:100 immediately prior to freezing to reduce background. Scale bars = 100 nm. (B) Representative X-ray diffraction spectra of MMT and LAP nanoplatelets in 20% dextran−aldehyde or 24.6% dendrimer; the presence of a peak indicates nanoplatelet stacking and a lack of complete exfoliation. (C) Varying polymer−nanoplatelet ratios result in varying exfoliation; at high PAMAM concentration and low MMT concentration (6% MMT, 24.6% PAMAM), exfoliation appears complete, but as polymer concentration decreases or MMT concentration increases, increasing XRD signal is indicative of intercalated and tactoid structures. Vertical lines at each peak are labeled with the corresponding *d*-spacing, giving approximate interplatelet distances in angstroms.

(acrylamide), particularly for uses in membranes and controlled drug delivery systems.[25,32−34] Emerging research has proposed the use of nanoplatelet composite hydrogels containing phyllosilicates for clinical applications,[35−39] though there has to date been no systematic exploration of the effect of nanoplatelets on rheological and mechanical properties in injectable hydrogel systems.

We designed and evaluated the performance of phyllosilicate nanoplatelets in controlling the rheological and mechanical properties of a poly(amido amine) dendrimer−dextran aldehyde injectable hydrogel previously shown to exhibit promising biocompatibility and control over degradation and drug release.[40−42] Crucially, we compared different aspect ratio phyllosilicates with differently sized nanoparticulate fillers to probe the effects of size and shape on material properties, particularly those important for enhancing the applicability of injectable hydrogels in challenging implantation environments. A compound nanocomposite composed of a mix of different aspect ratio nanoplatelets allowed for nearly independent tuning of rheological and mechanical properties, with substantial improvements over similarly sized nanoparticles. Using these data, we arrive at a mechanistic model of how different aspect ratio nanoplatelets affect material properties, with important lessons for the design of clinically relevant injectable nanocomposite hydrogels.

RESULTS AND DISCUSSION

Morphology of Nanocomposites. We prepared macromer solutions of dextran aldehyde and a poly(amido amine) (PAMAM) dendrimer with four different nanoscale fillers. Two fillers were phyllosilicate nanoplatelets with differing aspect ratios: a purified, naturally derived montmorillonite (MMT) with a thickness of 1 nm and lateral dimensions on the order of hundreds of nanometers, and a pH-stabilized synthetic hectorite (sodium magnesium fluorosilicate) commercially available as Laponite XL21 (LAP), with 1 nm thickness and 20−30 nm lateral dimensions. We compared these nanoplatelets to two nanoparticulate fillers: carbon black (CB), with a stated diameter of 30 nm, and nanoparticulate hydroxyapatite (nHAp), with a stated diameter of less than 200 nm.

DOI: 10.1021/acsnano.6b06730
ACS Nano 2017, 11, 2598−2610

Phyllosilicate nanoplatelets affect material properties profoundly when fully exfoliated in the polymer phase.[27] Typically, composites of nanoplatelets and hydrophilic polymers have been achieved by dispersion of nanoplatelets in monomer solutions followed by polymerization around the exfoliated platelets.[43] In contrast, we chose to exfoliate nanoplatelets directly in functionalized macromer solutions in order to achieve a high degree of control over macromer structure and functionalization. After dispersal in macromer solutions overnight (Figure 1A), exfoliation was evaluated by X-ray diffraction (XRD) and cryo-TEM (Figure 2). The two nanoplatelets showed a preference for different polymers: low aspect ratio LAP dispersed fully only in dextran aldehyde, whereas high aspect ratio MMT dispersed better in PAMAM dendrimer (Figure 2B). XRD confirmed the TEM imaging, with poorly exfoliated nanoplatelets (*e.g.*, LAP in PAMAM dendrimer and MMT in dextran aldehyde) showing a broad diffraction peak at 5.5° (dextran/MMT) and 6° (PAMAM/LAP), corresponding to *d*-spacing of 16.1 and 14.7 Å respectively, but little to no discernible peak for well-exfoliated samples. Conversely, CB and nHAp nanoparticles chosen as nanofiller controls appeared to aggregate in the polymer solutions despite extensive attempts at dispersion using sonication and agitation.

TEM imaging confirmed literature values for the shape and size of nanofiller samples (Figure 2A). LAP nanoplatelets were ∼1 nm thick and ∼20−30 nm in lateral dimension. MMT nanoplatelets were also ∼1 nm thick but had lateral dimensions of 100−200 nm. CB nanoparticles appeared roughly spherical with diameters of 30−50 nm, though some samples also showed a second population of much smaller particles (∼10 nm). nHAp nanoparticles appeared perfectly round with a wide range of diameters reaching as high as 100 nm.

These morphologies allowed for the controlled comparison of different properties across the different fillers; CB and nHAp nanoparticles exhibited surface areas on the order of 250 and 10 m^2/g, respectively.[44,45] The surface area of Laponite XL21 is estimated at ∼900 m^2/g.[46] The surface area of MMT as determined by the methylene blue method is approximately 1100 m^2/g.[47] LAP and MMT samples thus exhibited similar surface areas and densities, but lateral dimensions of MMT nanoplatelets were approximately 1 order of magnitude larger than LAP platelets. Based on a geometric approximation, we estimate that, for a given gram of LAP, there are approximately 2 orders of magnitude more platelets and 1 order of magnitude higher edge-to-face ratios compared to a gram of MMT.

It is important to note that while the chemistry of MMT and LAP differs slightly, the surface chemistry (tetrahedral silicon oxide crystals) is identical; the substitutions in the central octahedral layer comprise the major chemical distinction between the two nanoplatelets. As we expected the exfoliation, rheology, and mechanics emerging from these nanocomposites would be largely dictated by surface interactions, we hypothesized that it would provide us with the ability to isolate the effects of aspect ratio on nanocomposite properties.

Degree of exfoliation was dependent on the polymer/nanofiller ratio: higher concentrations of polymer and lower concentrations of nanoplatelets achieved better exfoliation, as demonstrated with PAMAM and MMT (Figure 2C). This suggests an upper limit on effective MMT loading in the 6−10% range, consistent with previous work.[27] Higher concentrations of nanoplatelets manifested as a mix of intercalated and exfoliated platelets. We were unable to determine an upper limit for LAP exfoliation as loading levels in excess of 6% were impossible to achieve due to rapid buildup of viscosity making dispersion of additional LAP impractical.

Phyllosilicate nanoplatelets will, to a degree, self-exfoliate in water, due to solvation effects of water on the cations between nanoplatelets. This effect is limited to relatively low concentrations of nanoplatelets and is not stable; at any given time, a dispersion of nanoplatelets in water will contain a mix of exfoliated and stacked structures. The addition of macromers to the dispersion serves to stabilize exfoliated nanoplatelets in solution, preventing reaggregation through either competitive binding (*i.e.*, polymer−platelet interaction inhibiting restacking) or stabilization of platelet−platelet structures (*e.g.*, edge-to-face interactions of platelets that prevent aggregation). This allows for a greater degree of exfoliation at higher concentrations of platelets; the polymer/platelet ratio provides a limiting factor on how much nanoplatelet can be consistently exfoliated, as evidenced by Figure 2C.

These stabilization phenomena are not well-characterized, but among other things, they are dependent on polymer charge/polarity, shape, and availability of functional groups for interaction with nanoplatelets. Work by Aida and colleagues focused on the use of dendritic and linear guanidinium and poly(ethylene) oxide (PEO)-based molecular binders in creating supramolecular gels with Laponite XLG, a synthetic hectorite. They demonstrate that both linear and dendritic molecules are capable of interacting with phyllosilicate nanoplatelets but that important determinants of the resultant interaction were driven by the number of functional groups (in this case, cationic guanidinium) available for binding and the size and flexibility of the PEO linker.[48] In this context, we hypothesized that stronger (ionic) polymer−platelet bonding might benefit MMT stabilization in an exfoliated state given its larger size and concomitant larger thermodynamic preference for a stacked morphology; the positively charged amine groups on the dendrimer surface afforded better stabilization in an exfoliated state. The physical size of each dendrimer (∼5 nm) may also have helped to physically separate nanoplatelets that were in the process of aggregation.

Strength of bonding between polymers and platelets is not the only factor, however; morphology and the availability of polymer for binding mattered, as well. With the much larger number (100×) of LAP platelets in a given gram of nanoplatelets compared to MMT, more polymer−platelet bonds are needed to stabilize most of the nanoplatelets in an exfoliated state. The large, inflexible, and roughly spherical structure of dendrimers "wastes" a lot of polymeric weight inside the dendrimer that is not available for stabilizing nanoplatelets; furthermore, the shape places some steric limitations on the number of nanoplatelets that can conceivably bind to a single dendrimer, limiting their contribution to a polymer−platelet network structure that can further stabilize nanoplatelets in an exfoliated state. Nevertheless, the role of steric effects with respect to the shape and size of additives to nanoplatelet dispersions is quite complex and still unclear.[49] We further hypothesized that for smaller and more numerous nanoplatelets, a flexible, more linear macromer such as dextran aldehyde would allow for comprehensive polymer−platelet interactions that could better stabilize LAP in an exfoliated state.

Bingham Fluid Properties of Nanofiller Dispersions. Macroscopically, the macromer−phyllosilicate nanoplatelet solutions appeared to exhibit flow properties substantially different than those of macromer solutions alone, with dramatic

DOI: 10.1021/acsnano.6b06730
ACS Nano 2017, 11, 2598−2610

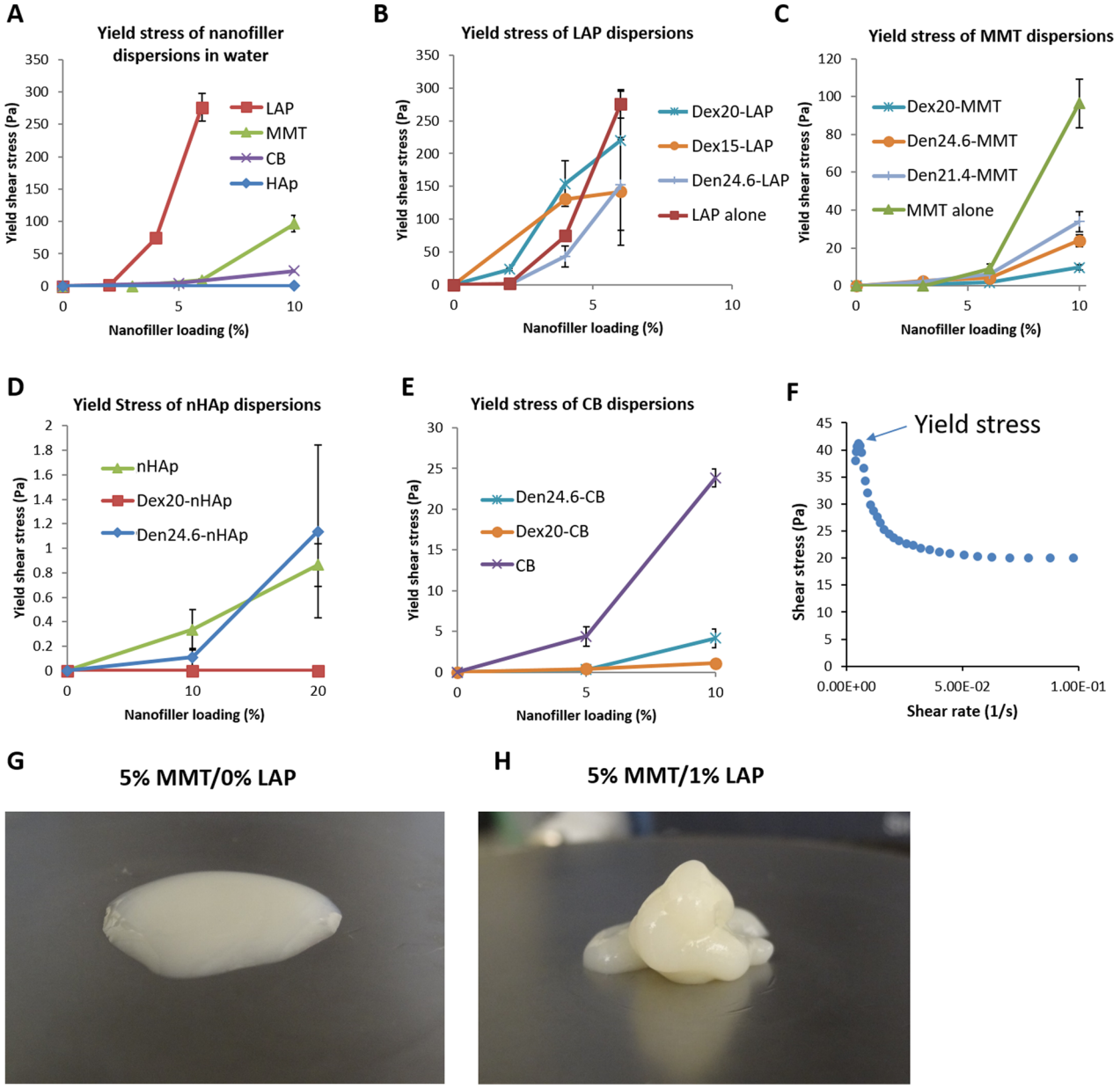

Figure 3. Yield shear stress of nanofiller dispersions in water (A) and macromer solutions (B–E); Dex20 denotes a 20% solution of dextran aldehyde, and Den24.6 denotes a 24.6% solution of PAMAM dendrimer. Note the substantially different scaling on the *y*-axis between each graph. LAP dispersions rapidly developed high yield stresses at very low concentrations (up to ~300 Pa at 6% loading); MMT dispersions also developed high yield stresses but only at higher loading (up to ~100 Pa at 10% loading). Nanoparticulate comparators CB and nHAp showed much smaller increases in yield shear stress (up to 30 and 1 Pa at 10 and 20% loading, respectively). (F) Sample plot taken of 2% LAP in 20% dextran showing an initial peak in shear stress at very low shear rates followed by a drop to an equilibrium value. The initial peak was used for calculating yield shear stresses. Qualitatively, when handling 20% dextran with and without 2% LAP mixed with 24.6% dendrimer with 10% MMT, the difference in handling properties was profound. In the absence of LAP (G), the mixture flowed readily into a small "puddle"; with the addition of low concentration LAP (H), the solution held its shape upon extrusion and could be layered and manipulated.

changes in viscosity and apparent Bingham fluid behavior. Previously published work suggests a number of potential mechanisms for rheological changes evident in nanoplatelet dispersions. LAP and other phyllosilicates have been hypothesized to form a "house of cards" structure of interactions between positively charged edges with negatively charged faces.[50,51] Alternatively, some have argued that nanoplatelets form a "Wigner glass" in solution, where the highly charged faces repel each other, forming a temporary gel. These mechanisms are substantially affected by nanoplatelet loading, ionic strength, and pH.[52] Many of the mechanistic studies carried out to support either model were at substantially lower concentrations and did not include the presence of macromer molecules to complicate matters; however, the higher concentrations may favor an attractive "house of cards" morphology over a repulsive Wigner glass.[53−55] More theoretically, sol−gel transitions in clay dispersions and the resultant rheological properties are tied to the concentration at which the effective hydrodynamic volume of the nanoplatelets begins to overlap; the role of macromers or other additives in modifying this behavior adds substantial complexity. Since the ratio of the hydrodynamic volume to actual volume is highest

DOI: 10.1021/acsnano.6b06730
ACS Nano 2017, 11, 2598−2610

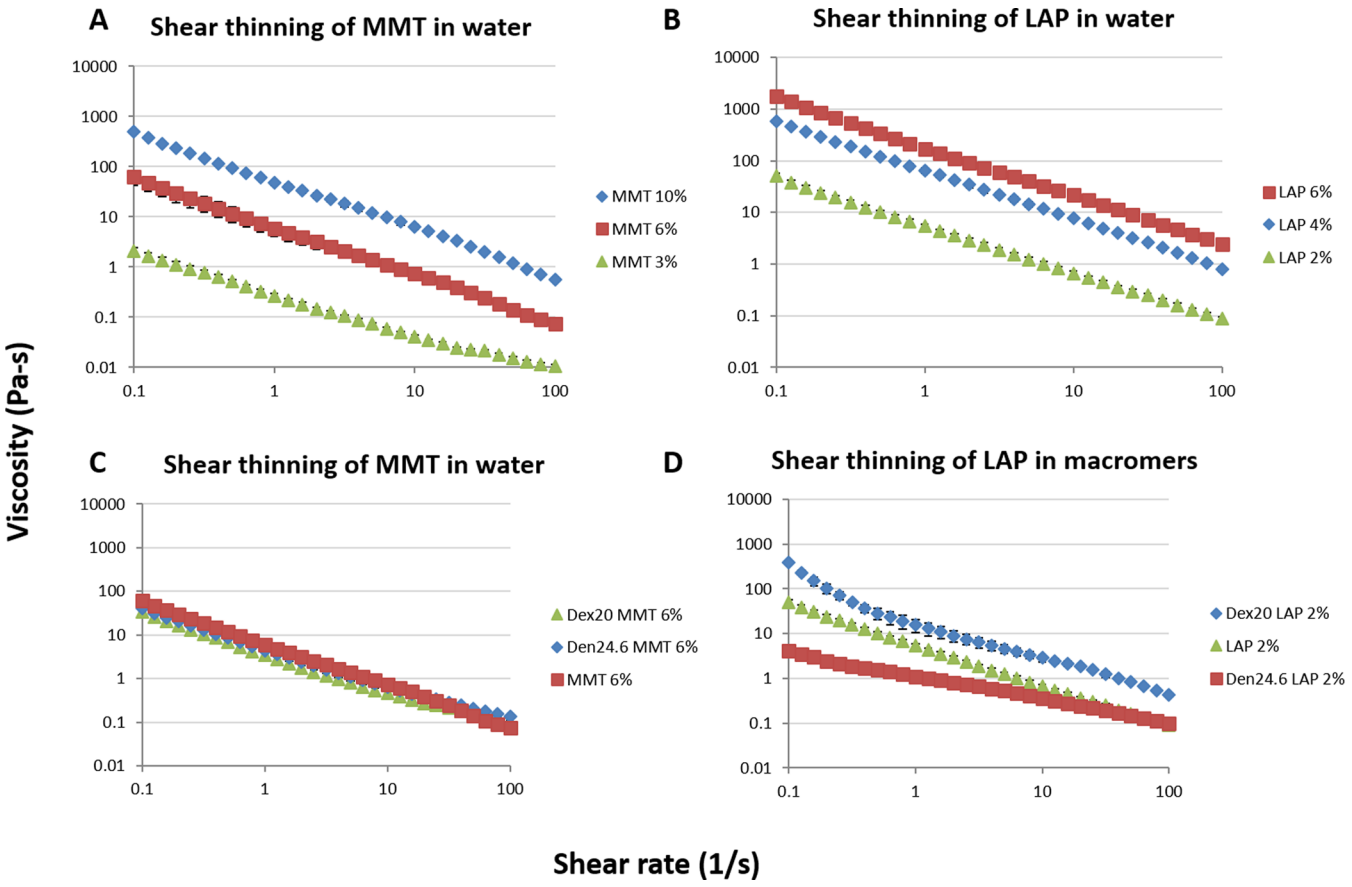

Figure 4. Shear thinning properties of nanoplatelet dispersions. Both MMT (A) and LAP (B) were dispersed in water and tested for equilibrium viscosity over shear rates spanning 3 orders of magnitude. When dispersed in macromer solutions (Dex20 = 20% dextran, Den24.6 = 24.6% dendrimer), MMT did not appreciably change shear thinning behavior (C), but LAP showed substantial changes in viscosity and degree of shear thinning depending on the choice of macromer (D).

with nanoplatelets, this mechanism does not extend as well to nanoparticulate fillers.[49,56,57]

Irrespective of the precise mechanism, these noncovalent filler−filler interactions as well as potential filler−polymer interactions allow nanoplatelet dispersions to behave like elastic solids below a yield stress; once these interactions are disrupted above the yield stress, the fluids can flow freely. In addition, continual re-forming of filler−filler−polymer interactions can impart substantially higher viscosities at low shear rates, which decrease at high shear rates due to the rate of noncovalent bond formation; this imparts shear thinning properties. Alternatively, higher shear rates may induce alignment of nanoplatelets in the direction of flow, reducing viscosity.[58] We evaluated the yield stress startup behavior and the shear thinning behavior of nanofiller dispersions in different macromer solutions.

Nanofillers dispersed in water showed rapid increases in yield stress at low loading for LAP, reaching as high as ∼300 Pa at 6% loading. MMT dispersions in water exhibited similar increases at higher loading levels. CB loading resulted in a substantially smaller yield stress, while nHAp appeared to have no meaningful effect up to 10% loading (Figure 3A).

When loaded into macromer solutions, yield stress behavior remained broadly similar, though with some modifications depending on the macromer. LAP loading in dextran increased yield stress over dispersion in water at 2 and 4% loading but decreased yield stress at 6% loading, possibly due to incomplete dispersion at high filler concentrations. Dispersion in dendrimer resulted in uniformly lower yield stress, likely due to poor exfoliation (Figure 3B). MMT loading in polymers decreased yield stress compared to water at 10%. Dextran−MMT solutions exhibited no increase in yield stress when compared with dispersions in water (Figure 3C).

Yield stress of CB and nHAp solutions was lower than that in nanoplatelet dispersions, though there were some minor variations with macromer solution. CB yield stress in macromer solutions was nearly zero, eliminating the modest yield stress (up to ∼30 Pa) observed in water solutions. nHAp solutions resulted in marginally higher yield stresses when dispersed in water or dendrimer compared to dextran, but all nHAp solutions were uniformly low yield stress (∼1 Pa or lower) (Figure 3D,E).

Overall, these data suggest that nanoplatelets caused profound changes in yield stress behavior of macromer solutions, with the strongest effect seen with LAP in dextran solutions at low loading. MMT loading also increases yield stress but only at higher volume fraction. When evaluated qualitatively, addition of small amounts of LAP to macromers caused dramatic improvements in handling, allowing for layering and sculpting the material prior to polymerization (Figure 3G,H).

Shear Thinning Properties of Nanofiller Dispersions. Nanoplatelet dispersions in water exhibited strong shear thinning properties, with viscosities decreasing by ∼3 orders of magnitude across the range of shear rates tested. Viscosity of LAP dispersions was substantially higher than that in MMT dispersions, with 6% LAP having a peak viscosity of 1788 Pa-s

DOI: 10.1021/acsnano.6b06730
ACS Nano 2017, 11, 2598−2610

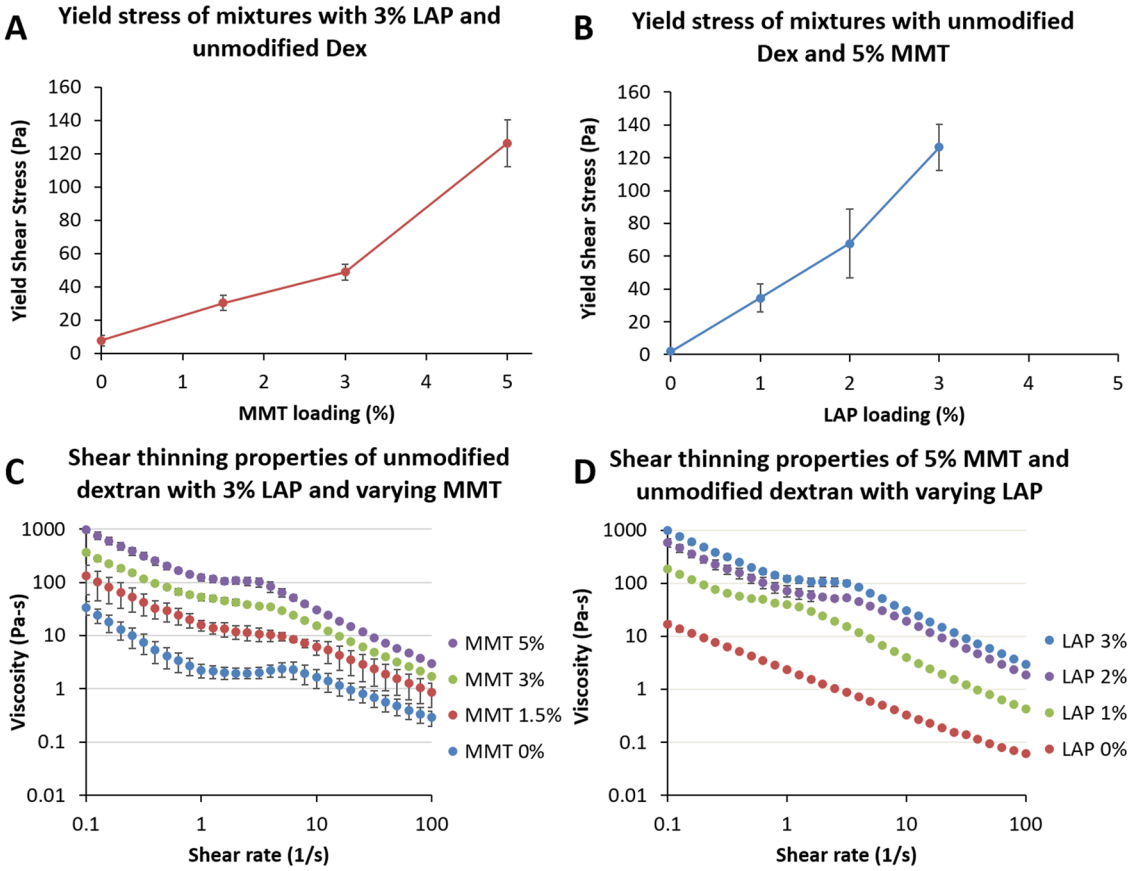

Figure 5. Rheological characterizations of polymer mixtures. Rheological characterization of the combination of dextran−LAP and dendrimer−MMT were approximated using unoxidized dextran in order to prevent cross-linking during rheological study. (A,C) Fixed concentration of 6% LAP in 20% dextran was mixed 1:1 with 24.6% dendrimer containing varying MMT content at pH ∼9.2 (upon mixing, the final concentrations were halved and are represented in the legends). (B,D) Fixed concentration of 10% MMT in dendrimer was mixed 1:1 with 20% dextran containing varying LAP content. The addition of increasing MMT content does not disrupt LAP−LAP and LAP−dextran interactions but rather further enhances rheological behavior.

while 6% MMT only achieved 63 Pa-s (Figure 4A,B). Dispersions of hydroxyapatite and carbon black both exhibited shear thinning behavior, though nHAp viscosities were uniformly low (<10 Pa-s) and of little value in changing handling properties (Supplemental Figure 1).

When dispersed in macromer solutions, dispersions of MMT exhibited very similar shear thinning properties compared to dispersions in water. Both dextran and dendrimer solutions appeared to slightly reduce the magnitude of the maximum viscosity, but the shear thinning behavior was largely unchanged. Interestingly, dispersion of LAP in macromer dispersions caused more substantial changes to shear thinning behavior. LAP−dextran dispersions exhibited uniformly higher viscosities than water dispersions, suggesting a synergistic effect, with platelet−polymer interactions adding to already existing platelet−platelet interactions. Conversely, LAP−dendrimer dispersions exhibited substantially decreased shear thinning behavior and viscosities, possibly due to the aforementioned poor LAP exfoliation in dendrimer solutions (Figure 4C,D).

The observed differences between LAP and MMT are instructive; though they have similar structures, LAP has a significantly smaller aspect ratio (∼20:1) compared to that of MMT (∼100−200:1). The higher number of platelets (100×) and increased edge-to-face ratio (10×) allows for more platelet−platelet−polymer interactions in a given concentration and volume, increasing yield stress and viscosity.[59] This may be partially due to changes in "hydrodynamic trapping" behavior that scales with particle size, though the reality is likely more complex.[60] Furthermore, the observed synergy with dextran aldehyde suggests that dextran−LAP interactions play a key role in enhancing rheological properties. The dendrimer−LAP data help confirm this hypothesis; the demonstrated poor exfoliation of LAP in the dendrimer may be from poor dendrimer−LAP interactions, which substantially limit the formation of these noncovalent associations during flow. These data demonstrate the importance of matching polymer choice with a given nanofiller to achieve optimal dispersion and efficacy.

Nanoparticles such as carbon black and hydroxyapatite, conversely, have substantially lower surface area available for interactions given the same weight of filler; most of the filler volume is "wasted" inside the center of each particle. Although smaller diameter nanoparticles will have better surface area to volume ratios, each particle will only have limited scope for interaction with other particles due to steric hindrance; generation 5 PAMAM dendrimers, for example, are ∼5 nm in diameter, meaning that the available sites for interaction on a single ∼30 nm nanoparticle are limited. Nanoplatelets, in contrast, have substantially more availability given their higher surface area and shape, in agreement with previous simulations and highly controlled experiments.[61] Furthermore, the homogeneous surface chemistries of most nanoparticles do

DOI: 10.1021/acsnano.6b06730
ACS Nano 2017, 11, 2598−2610

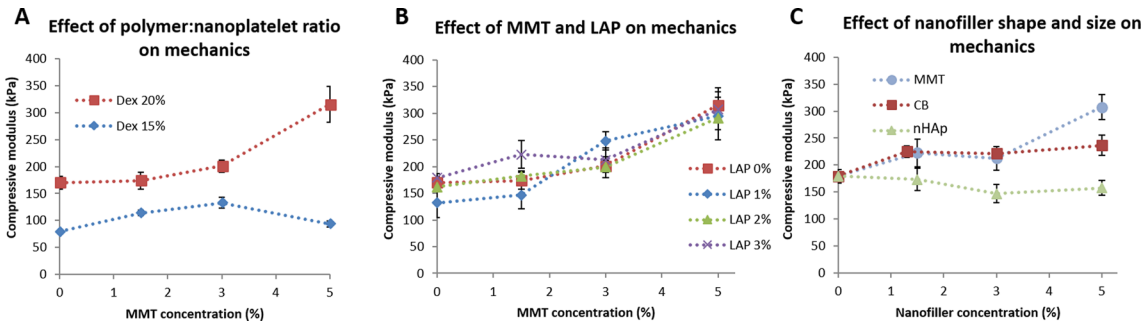

Figure 6. Mechanical reinforcement of nanocomposite hydrogels. (A) Effects of overall macromer content on mechanics as a function of MMT concentration. Two macromer contents with identical dextran/dendrimer ratios (20% dextran/24.6% dendrimer and 15% dextran/18.5% dendrimer) were tested with 3% LAP and a range of MMT loading. Nanofiller content is reported as final concentration in the hydrogel; concentration in the individual macromer solutions was doubled due to 1:1 mixing. (B) MMT and LAP loading were varied from 0 to 5% and 0 to 3%, respectively, in constant 20% dextran and 24.6% dendrimer macromer solutions. (C) Nanoparticulates CB and nHAp were tested at 0−5% loading compared to MMT. All hydrogels contained 3% LAP.

not allow for dissimilar edge−face interactions as proposed for phyllosilicate nanoplatelets.

Both high yield stresses and shear thinning properties are desirable for injectable materials in wet or inverted environments. The relatively high shear rates and shear stresses in a syringe will readily allow for injection into the implantation site, but the low shear stresses and shear rates seen in the site will allow the material to stay in place during cross-linking rather than flowing away. The rheological properties of LAP−dextran dispersions appear well-suited to achieving these properties at very low loading of nanofiller (≤6%).

Rheological Properties of Mixtures. Rheological properties of complete mixtures of dextran−aldehyde/LAP and PAMAM dendrimer/MMT could not be determined quantitatively due to the short gelation time (~1 min) precluding a thorough analysis of transient handling properties. Qualitatively, we observed that small changes in LAP content caused substantial changes in handling performance, but similar changes in MMT content had a more subdued effect; for a given MMT content chosen (in order to provide mechanical reinforcement), a wide range of rheological properties could be achieved by varying LAP content. However, in order to provide quantification of these observations, we prepared mixtures of unoxidized dextran/LAP and PAMAM dendrimer/MMT; the dextran, lacking in aldehyde groups, did not react with the PAMAM dendrimer, leaving a stable solution for analysis. While unoxidized dextran is not expected to have nanoplatelet interactions and exfoliation behavior identical to that of the dextran aldehyde, this study was performed merely to understand whether the addition of MMT to the system substantially disrupted the rheological properties observed with dextran/LAP alone.

A fixed concentration of 6% LAP in 20% dextran was mixed 1:1 with 24.6% dendrimer containing varying MMT content at pH ~9.2 (upon mixing, the final concentrations were halved and are represented in Figure 5A,C). A fixed concentration of 10% MMT in 24.6% dendrimer was mixed 1:1 with 20% dextran containing varying LAP content (Figure 5B,D). As expected, there was a dose-dependent increase in yield shear stress and viscosity with increasing MMT content, suggesting that MMT does not interfere substantially with the LAP-mediated rheological properties, instead reinforcing them. This matched our qualitative observations, where small changes in LAP content could cause large effects on handling properties, allowing for fine-tuning. Previous work from the study of mixtures of LAP and MMT dispersions in water (without the addition of macromers) indicates that LAP interactions dominate over MMT and may enhance MMT stability in forming cooperative gel networks.[62−64]

Although the single nanoplatelet solutions were tested to relatively high loading concentrations (6 and 10% for LAP and MMT, respectively), the final concentrations upon mixing the two macromer solutions were half of the original concentration. This provides an upper limit for nanoplatelet loading based on the maximal loading possible for well-exfoliated nanoplatelets in individual macromer solutions. While this may in theory be a limitation on the rheological properties attainable, in practice, we found that the handling properties of final solutions containing 2−3% LAP were more than sufficient for application in submerged, flowing, and inverted implantation environments. If needed, one could further optimize LAP dispersion in both macromer solutions to provide maximal rheological performance, though we did not find this to be necessary.

Mechanical Properties of Nanocomposite Adhesive Hydrogels. Given the exfoliation preference of nanoplatelets, dextran aldehyde was paired with LAP while PAMAM dendrimer was paired with MMT. Solutions of macromer and dispersed nanoplatelets were mixed using a static mixer and allowed to polymerize (Figure 1B). Gelation time was highly dependent on the pH of the dendrimer−MMT dispersion due to the protonation state of primary amines; gelation time could be tuned from seconds to minutes as necessary (Supplemental Figure 2), allowing for a range of handling times as dictated by clinical necessity. As this can also affect the final degree of cross-linking, an intermediate pH and gelation time was chosen for all further studies.

We initially attempted to study nanofiller effects on mechanical properties individually; however, the substantial viscosity differences between macromer solutions with and without nanofiller precluded complete mixing. Complete mixing of macromer solutions was crucial for achieving good cross-linking, and poor cross-linking arising from rheological mismatches overwhelmed any differences that might be discerned from changes in nanofiller content. As such, we evaluated the combination of LAP−dextran with dendrimer doped with the other three nanofillers to determine if the improved rheological properties from LAP−dextran dispersions could be combined with the improved compressive stiffness of other nanocomposites. Compressive modulus was evaluated at two different overall polymer weights while keeping the

DOI: 10.1021/acsnano.6b06730
ACS Nano 2017, 11, 2598−2610

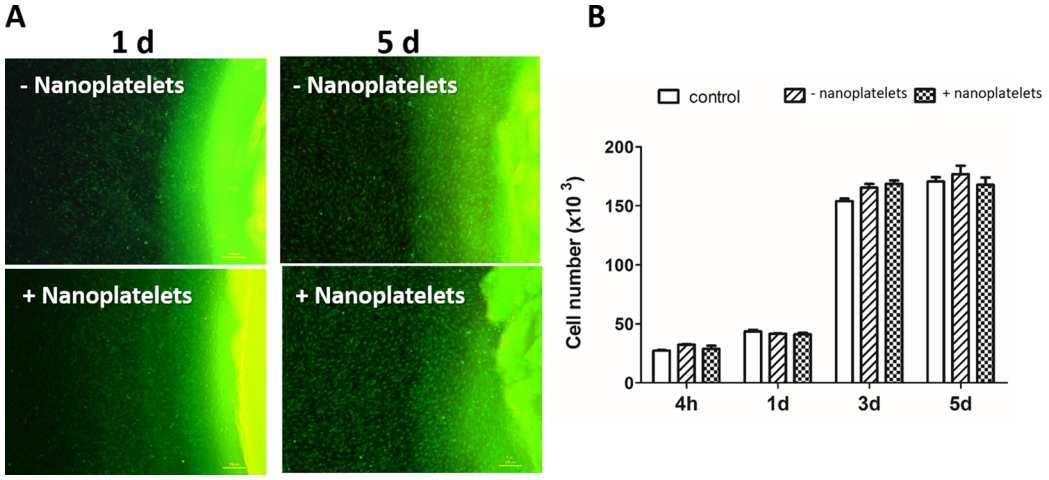

Figure 7. Cytocompatibility of nanocomposite hydrogels. (A) C3H10T1/2 mouse mesenchymal cells were tested in culture in direct contact with hydrogels with and without nanoplatelets. Final hydrogel content was 10% dextran aldehyde, 2% LAP, 12.3% dendrimer amine, and 3% MMT. Following 1 and 5 days in direct contact with the hydrogels, cells were assayed for viability by live (green)/dead (red) staining; the hydrogel, visible at the right of each image, is also stained green. (B) Cell proliferation and viability was quantified by the PrestoBlue assay over 5 days when compared to untreated control cultures.

dendrimer/dextran ratio constant (Figure 6A). High polymer content hydrogels showed an increase in modulus with fixed LAP and increasing MMT concentration. Lower polymer content gels, however, exhibited no significant change in modulus with increasing MMT loading. We hypothesize that the poor exfoliation of MMT in lower polymer content (see Figure 2) was responsible for the apparent ineffectiveness of MMT loading, underlining the need for well-exfoliated nanoplatelets for maximal material effects. Furthermore, we evaluated compressive modulus of LAP–MMT nanocomposites across a range of LAP and MMT concentrations (Figure 6B). Across the range of conditions, increasing LAP content in hydrogels had little effect on compressive modulus despite excellent exfoliation and polymer–filler interactions.

To compare the effects of nanofiller shape on compressive reinforcement, we studied the effects of increasing CB and nHAp content in nanocomposites containing fixed LAP concentration (Figure 6C). Increased nHAp content had no significant effect on hydrogel modulus up to 5% loading, whereas increased CB content modestly increased modulus (5% CB increased modulus ~32% over hydrogels with no CB). In comparison, MMT at the same concentration reinforced compressive modulus by ~72%.

We speculate that the difference between MMT and LAP effects on compressive stiffness can be attributed to the varying aspect ratio between the two nanofillers. MMT, being a much larger platelet than LAP, allows for many more potential filler–polymer associations per platelet. This increased number of noncovalent "cross-links" at each node allows for the stiff platelets to strengthen the hydrogel more effectively than the more diffuse cross-linking network of LAP.

MMT, however, was able to achieve substantial increases in compressive modulus at much lower loading ratios than seen in nanoparticulate fillers. We speculate that this is from the increased surface area to volume ratio of nanoplatelets as well as enhanced polymer–filler interactions. Clearly, dispersion of nanofillers is of critical importance to optimal stiffening of materials; poorly exfoliated tactoids of MMT, which more closely mimic nanoparticles in shape and size, had little to no effect on compressive modulus at low loadings. Careful choice of formulation conditions to optimize nanofiller dispersion and filler–polymer interactions is thus of great importance.

These data suggest that well-exfoliated MMT has a strong influence on the compressive modulus of hydrogel nanocomposites at low loading ratios, while LAP has a much stronger effect on rheological properties. This allows for nearly independent tuning of mechanical and rheological properties of nanocomposite hydrogels; injection and handling properties can be tweaked to meet clinical needs without substantially harming the mechanical performance of the final material. Importantly, the combination of MMT and LAP enables lower overall filler loading while achieving the desired rheological and mechanical properties; low loading ratios decrease the impact of fillers on other hydrogel properties, including high water content and biocompatibility.

Cytocompatibility of Nanoplatelet Nanocomposite Materials. To validate the potential of nanoplatelet nanocomposite hydrogels in a clinical context, hydrogels were tested for *in vitro* cytocompatibility. Mouse mesenchymal cells were cultured in direct contact with dextran/dendrimer hydrogels with and without nanoplatelets and assessed for cell death (by live/dead staining) and proliferation (by PrestoBlue assay) over 5 days (Figure 7). All conditions showed minimal cell death and excellent metabolic activity when compared to untreated controls.

A wide variety of other studies have demonstrated cytocompatibility of phyllosilicate-containing materials with different cell types, though some studies performed with nanoplatelet dispersions in the absence of any polymeric matrix have shown some dose-dependent toxicity that may be dependent on aspect ratio.[35,37,65−68] *In vivo* biocompatibility data are still scant, though some early studies have shown encouraging results.[34] These data suggest that phyllosilicate nanoplatelet nanocomposite hydrogels may be biocompatible, though a thorough investigation of *in vivo* behavior is necessary to determine the fate of implanted phyllosilicates.

Evaluation of Handling Properties. To demonstrate that the enhanced properties of these materials could be used in challenging implantation environments, we injected the material into submerged osteochondral defects in a mock

DOI: 10.1021/acsnano.6b06730
ACS Nano 2017, 11, 2598–2610

arthroscopic setting. Macromer solutions alone were rapidly dispersed in the surrounding fluid following injection. Nanoplatelet composite materials, however, were easily retained in the defect space and could be shaped to fit the contours of the defect (see the video in the Supporting Information). The presence of fluid flow did not cause the material to deform or disperse in solution due to the high yield stress and viscosities of the material at low shear rates, yet the material could be easily injected and shaped. These data suggest that this nanocomposite hydrogel may be an ideal injectable vehicle for challenging implantation environments.

In addition to the demonstrated benefits of mixed aspect ratio nanoplatelet hydrogels, we expect that nanoplatelets would allow for greater tunability over other aspects of a drug delivery system. Importantly, the high surface area of nanoplatelets compared to other nanofillers changes the ways in which hydrogels degrade and elute drugs. High aspect ratio nanoplatelets such as MMT may act as diffusion barriers to drugs and degradation byproducts, allowing for selective tuning of degradation and drug release. Furthermore, the nanoplatelet−polymer interactions may directly impact material degradation through creation of a secondary noncovalent network that enhances hydrogel stability. The large surface area available also provides potential sites for immobilization of drugs or other biologically important moieties. These proposed advantages of nanoplatelet nanocomposites must be evaluated in future studies.

We demonsrate a mix of different aspect ratio nanoplatelets to achieve nearly independent enhancement of rheological and mechanical properties in a hydrogel. MMT and LAP have been compared before; for example, rheological and aging characteristics of their dispersions in water were described in some detail. These studies, however, involved highly controlled conditions to elicit theoretical understandings of dispersion dynamics. Fully realized materials have chosen a single nanofiller to enhance a desired property without attempting to understand the underlying effects of particle size and shape. Here, we demonstrate that fine levels of control can be achieved using a mix of different nanoplatelets at low overall loading (typically 8% or less).

More importantly, we introduce a conceptual framework to use in the design and evaluation of nanoplatelet nanocomposites. Choice of polymer is critical: achieving homogeneous dispersions and strong polymer−platelet interactions dramatically improves exfoliation, increasing the contribution of nanoplatelets to modifying material properties. Controlling these interactions through surface modification or changes to solvent properties can have profound effects on nanocomposite functionality. Furthermore, shape and surface area of nanoplatelets matter: conventional nanoparticles were not able to achieve the same control over material properties at the very low concentrations used. When using nanoplatelets, rheological modifications appear to be driven primarily by platelet−platelet interactions and as such are more effective with a finely grained network of small aspect ratio nanoplatelets such as LAP. Conversely, mechanical reinforcement critically relies upon the polymer−platelet interface, with considerations of sterics and the size of cross-linking nodes gravitating toward larger aspect ratio nanoplatelets for maximal effect. This framework will help inform the design of future nanocomposites, whether or not they are based on phyllosilicate nanoplatelets.

CONCLUSIONS

Nanoplatelet nanocomposites can contribute greatly to the design of systems with controlled mechanics and injectability and find many potential clinical uses. While control nanoparticulate fillers may have only modest effects on rheological and mechanical tuning of hydrogels, phyllosilicate nanoplatelets impart substantial changes to material properties at very low overall loading (<10%). Control over aspect ratio of nanoplatelets provides nearly independent tuning of rheology and mechanics, with lower aspect ratio LAP finely tuning rheological properties and high aspect ratio MMT reinforcing mechanical modulus. This mix of different aspect ratio nanoplatelets produces a broadly tunable nanocomposite hydrogel with the ability to be implanted in wet, flowing, and inverted environments. This system can be readily tuned across a large parameter space and may provide a useful platform material for drug delivery applications in a range of implantation environments and applications.

MATERIALS AND METHODS

Preparation of Macromer Solutions. Dextran aldehyde with ∼50% aldehyde substitution was prepared by periodate oxidation of dextran (Pharmacosmos, 10 kDa) as previously described.[40] Oxidation degree was confirmed by a hydroxylamine hydrochloride titration assay.[69] Lyophilized dextran−aldehyde was reconstituted in 1 mL of water to the desired concentration (typically 200 mg/mL). Similarly, generation 5 poly(amidoamine) dendrimers with 25% amine surface groups (Dendritech) were diluted to the desired concentration (typically 246 mg/mL), and concentrated hydrochloric acid was used to bring pH to the desired level (typically 9.2). When needed, nanofillers were added to each 1 mL macromer solution, immediately vortexed, and placed on a cell disruptor (Disruptor Genie, Scientific Industries) at 4 °C overnight (Figure 1A). Nanofillers tested included purified montmorillonite (MMT; Gelwhite H, a kind gift from Byk additives), a pH-stabilized synthetic hectorite (LAP; Laponite XL21, Byk), hydroxyapatite nanoparticles (nHAp, <200 nm, Sigma), and carbon black nanoparticles (CB, ∼30 nm, Graphene Supermarket). All nanofillers were used as received. Nanofiller content added was approximated as a percentage; that is, if 60 mg of nanofiller was added to 1 mL of macromer solution, this was approximated as a "6%" solution.

Characterization of Nanofiller Dispersion. Nanofiller dispersions were examined for degree of exfoliation and morphology by both cryo-transmission electron microscopy (cryo-TEM) and X-ray diffraction (XRD). For cryo-TEM, dispersions were diluted 1:100 in ultrapure water (to reduce background), after which 3 μL of sample was dropped on a lacey copper grid coated with a continuous carbon film and blotted to remove excess sample without damaging the carbon layer by Gatan Cryo Plunge III. The grid was mounted on a Gatan 626 single tilt cryo-holder equipped in the TEM column. The specimen and holder tip were cooled with liquid nitrogen, which maintains temperature during transfer into the microscope and subsequent imaging. Imaging on a JEOL 2100 FEG microscope was done using a minimum dose method that was essential to avoid sample damage under the electron beam. The microscope was operated at 200 kV and with a magnification in the ranges of 10 000−60 000 for assessing particle size and distribution. All images were recorded on a Gatan 2kx2k UltraScan CCD camera.

For X-ray diffraction, undiluted macromer solutions were drop-cast onto glass slides and allowed to dry. They were then loaded into a Panalytical X'Pert Pro X-ray diffractometer using 0.04 rad Soller slits, a 10 mm fixed mask, a programmable divergence slit, a programmable antiscatter slit, and a 0.02 mm nickel filter. XRD spectra were acquired using an "X'Celerator" detector with a 2.122° active length; data were analyzed using X'Pert Highscore Plus software (Panalytical).

Rheology. Undiluted macromer solutions were tested for rheological behavior using a TA Instruments AR2000 rheometer.

DOI: 10.1021/acsnano.6b06730
ACS Nano 2017, 11, 2598−2610

Solutions were pipetted onto a 25 mm parallel plate fixture and maintained at 25 °C using a Peltier heater. The gap distance was set to 1 mm, and the macromer solution was allowed to equilibrate for 5 min. Subsequently, two tests were carried out: a yield stress test to examine startup behavior and a shear thinning test. Briefly, the strain rate was slowly increased until the shear stress hit a peak and started to decrease; this initial peak in shear stress was treated as the yield stress (Figure 3F). Shear thinning tests imparted a constant shear rate to the solutions ranging from 0.1 to 100 s^{-1} and recorded the equilibrium viscosity. Data were analyzed in TA Data Analysis software.

Polymerization of Hydrogels and Mechanical Analysis. Following overnight dispersion, macromer solutions were loaded into two barreled syringes (Medmix) and mixed using a static mixer attachment with up to 16 mixing stages (Figure 1B). Materials were extruded into cylindrical rubber molds and allowed to cross-link for up to 20 min prior to analysis.

Gelation time was determined for mixtures of macromer solutions containing 20% dextran aldehyde with a dispersion of 6% LAP and 24.6% PAMAM dendrimer with a dispersion of 10% MMT. The pH of the dendrimer/MMT solution was varied from 8 to 10.25, and the macromer solutions were mixed in a static mixer and placed in a glass tube with a magnetic stirrer. Gelation was determined by the cessation of free mixing by the stirrer. Based on these results, an intermediate gelation time was chosen, at a pH of 9.2, for all further studies.

Mechanical properties of hydrogels were tested using unconfined compression on a low-load submersible mechanical tester (Biss). Briefly, material dimensions were measured with calipers, and hydrogels were then placed between two parallel platens submerged in phosphate buffered saline at room temperature and preloaded with 50 mN of force to ensure adequate contact. The hydrogel was then compressed at 0.01 mm/s to at least 50% strain (past the compressive failure point of the material). Force and displacement data were sampled at 10 Hz and analyzed in Excel and MATLAB. Sample geometry was used to calculate stress and strain; due to violations of the infinitesimal strain condition at such high strain testing, an approximation of the true stress was substituted in place of the engineering stress, following the method previously published for cartilage tissue, where the cross-sectional area was scaled by the stretch ratio.[70] Stress and strain were plotted, and modulus was calculated from the tangent at 30% strain to avoid variations in startup behavior (due to imperfectly flat samples) as well as behavior near failure while evaluating modulus at as high a strain as possible to mimic the high strain/stress environments seen in cartilage tissues.[70] Choosing a high strain value that was always below failure allowed for consistent comparisons across samples.

Mechanical properties were first evaluated as a function of total macromer content, keeping the ratio between dextran and dendrimer constant; 20% dextran with 24.6% dendrimer was compared to 15% dextran with 18.5% dendrimer. In all conditions, dextran solutions contained 6% LAP; MMT content in the dendrimer was varied from 0 to 10%. Care was taken to ensure that all dendrimer−MMT dispersions were at pH 9.2 by titration with concentrated hydrochloric acid.

Following this, the effects of MMT and LAP content were compared; 20% dextran and 24.6% dendrimer solutions were mixed with LAP and MMT from 0 to 6% and 0 to 10%, respectively. Finally, these were compared to CB and nHAp: a 6% LAP dispersion in 20% dextran was mixed with 24.6% dendrimer containing varying amounts of CB or nHAp, from 0 to 10%.

Cytocompatibility Studies. Cytocompatibility of nanoplatelet nanocomposite materials was evaluated to determine their potential for use in the clinic. Passage 4−6 C3H10T1/2 mouse mesenchymal cells (ATCC) were plated in 6-well plates at 10 000 cells/cm^2 and allowed to adhere overnight. One hundred microliter hydrogels (4% LAP dispersion in 20% dextran mixed 1:1 with a 6% MMT dispersion in 24.6% dendrimer) were prepared in sterile molds and placed in direct contact with the cell layer. These were compared to control hydrogels without any nanofillers. The cells were cultured in 4 mL of growth medium (DMEM (Gibco) with 10% fetal bovine serum (Hyclone), 100 U/mL penicillin (Gibco), and 100 μg/mL streptomycin (Gibco)). Medium was changed three times weekly.

Following 1 and 5 days of culture in the presence of the hydrogel, the medium was aspirated and cells were stained for 30 min in 500 μL of live/dead solution (ThermoFisher) at room temperature. The cells were imaged using a Nikon Eclipse Ti fluorescence microscope in the FITC channel (green, calcein AM for viable cells) and the TRITC channel (red, ethidium homodimer-1 for dead or dying cells).

Proliferation of cells was measured using a Transwell assay. Cells were plated in 6-well plates at 2000 cells/cm^2, allowed to adhere overnight, and 100 μL hydrogels with and without nanoplatelets were placed above the cells in Transwell inserts; controls also included cells cultured without any material. Following culture for 4 h, 1 day, 3 days, and 5 days, inserts and medium were removed. Nine hundred microliters of fresh medium was added with 100 μL of PrestoBlue reagent (ThermoFisher), and cells were incubated for 30 min. Absorbance at 570 nm was read with a Varioskan Flash plate reader (Thermo Scientific) and compared against a standard curve of known plated cell numbers. Following measurement, media and inserts were replaced and cells were incubated until the next time point.

***Ex Vivo* Handling Evaluation in Porcine Knees.** Handling properties for injection and manipulation of hydrogels into tissue defects in wet environments was assessed qualitatively using an *ex vivo* osteochondral defect model. Porcine knees were obtained from a local butcher and were dissected to expose the cartilage of the distal femur. Cartilage defects were simulated using a 6 mm biopsy punch (Miltex), and knees were submerged in water. Under both static and flowing conditions, hydrogels with and without nanoplatelet fillers (20% dextran/6% LAP mixed 1:1 with 24.6% dendrimer/10% MMT; dye was added to either macromer solution for visualization) were injected into porcine knee defects, shaped to match the contours of the defect, and allowed to set.

ASSOCIATED CONTENT

Supporting Information

The Supporting Information is available free of charge on the ACS Publications website at DOI: 10.1021/acsnano.6b06730.

Underwater gelation of injectable hydrogel into a model osteochondral defect in a porcine knee (AVI)

Figures showing the shear thinning properties of carbon black and hydroxyapatite dispersions and pH dependence of gelation time (PDF)

AUTHOR INFORMATION

Corresponding Authors

*E-mail: unterman@mit.edu.

*E-mail: nartzi@mit.edu.

ORCID

Shimon Unterman: 0000-0003-0838-3635

Notes

The authors declare no competing financial interest.

ACKNOWLEDGMENTS

We are grateful for funding from Sanofi. We thank NIH R01 GM 49039 for funding. We thank the Koch Institute for Integrative Cancer Research at MIT for access to facilities, especially the Nanotechnology Materials Core Facility for rheometry and imaging needs. D.S. Yun was instrumental in obtaining cryo-TEM imagery. We thank the MIT Deshpande Center for Technological Innovation for support. We also acknowledge the MIT X-ray Diffraction Shared Experimental Facility for access to XRD equipment and thank S. Speakman for technical advice.

DOI: 10.1021/acsnano.6b06730
ACS Nano 2017, 11, 2598−2610

REFERENCES

(1) Vashist, A.; Ahmad, S. Hydrogels: Smart Materials for Drug Delivery. *Orient. J. Chem.* **2013**, *29*, 861−870.
(2) Blackburn, W. H.; Dickerson, E. B.; Smith, M. H.; McDonald, J. F.; Lyon, L. A. Peptide-Functionalized Nanogels for Targeted siRNA Delivery. *Bioconjugate Chem.* **2009**, *20*, 960−968.
(3) Peak, C. W.; Wilker, J. J.; Schmidt, G. A Review on Tough and Sticky Hydrogels. *Colloid Polym. Sci.* **2013**, *291*, 2031−2047.
(4) Hoffman, A. S. Hydrogels for Biomedical Applications. *Adv. Drug Delivery Rev.* **2012**, *64*, 18−23.
(5) Garg, T.; Singh, S.; Goyal, A. K. Stimuli-Sensitive Hydrogels: An Excellent Carrier for Drug and Cell Delivery. *Crit. Rev. Ther. Drug Carrier Syst.* **2013**, *30*, 369.
(6) Yang, J.-A.; Yeom, J.; Hwang, B. W.; Hoffman, A. S.; Hahn, S. K. In Situ-Forming Injectable Hydrogels for Regenerative Medicine. *Prog. Polym. Sci.* **2014**, *39*, 1973−1986.
(7) Li, Y.; Rodrigues, J.; Tomas, H. Injectable and Biodegradable Hydrogels: Gelation, Biodegradation and Biomedical Applications. *Chem. Soc. Rev.* **2012**, *41*, 2193−2221.
(8) Nguyen, Q. V.; Huynh, D. P.; Park, J. H.; Lee, D. S. Injectable Polymeric Hydrogels for the Delivery of Therapeutic Agents: A review. *Eur. Polym. J.* **2015**, *72*, 602−619.
(9) Markert, C. D.; Guo, X.; Skardal, A.; Wang, Z.; Bharadwaj, S.; Zhang, Y.; Bonin, K.; Guthold, M. Characterizing the Micro-Scale Elastic Modulus of Hydrogels for Use in Regenerative Medicine. *J. Mech. Behav. Biomed. Mater.* **2013**, *27*, 115−127.
(10) Calvert, P. Hydrogels for Soft Machines. *Adv. Mater.* **2009**, *21*, 743−756.
(11) Rodell, C. B.; Dusaj, N. N.; Highley, C. B.; Burdick, J. A. Injectable and Cytocompatible Tough Double-Network Hydrogels through Tandem Supramolecular and Covalent Crosslinking. *Adv. Mater.* **2016**, *28*, 8419.
(12) Sun, J.-Y.; Zhao, X.; Illeperuma, W. R. K.; Chaudhuri, O.; Oh, K. H.; Mooney, D. J.; Vlassak, J. J.; Suo, Z. Highly Stretchable and Tough Hydrogels. *Nature* **2012**, *489*, 133−136.
(13) Sun, T. L.; Kurokawa, T.; Kuroda, S.; Ihsan, A. B.; Akasaki, T.; Sato, K.; Haque, M. A.; Nakajima, T.; Gong, J. P. Physical Hydrogels Composed of Polyampholytes Demonstrate High Toughness and Viscoelasticity. *Nat. Mater.* **2013**, *12*, 932−937.
(14) Appel, E. A.; Tibbitt, M. W.; Webber, M. J.; Mattix, B. A.; Veiseh, O.; Langer, R. Self-Assembled Hydrogels Utilizing Polymer−Nanoparticle Interactions. *Nat. Commun.* **2015**, *6*, 6295.
(15) Rodell, C. B.; MacArthur, J. W.; Dorsey, S. M.; Wade, R. J.; Wang, L. L.; Woo, Y. J.; Burdick, J. A. Shear-Thinning Supramolecular Hydrogels with Secondary Autonomous Covalent Crosslinking to Modulate Viscoelastic Properties *In Vivo*. *Adv. Funct. Mater.* **2015**, *25*, 636−644.
(16) Moon, H. J.; Ko, D. Y.; Park, M. H.; Joo, M. K.; Jeong, B. Temperature-Responsive Compounds as In Situ Gelling Biomedical Materials. *Chem. Soc. Rev.* **2012**, *41*, 4860−4883.
(17) Yan, C.; Pochan, D. J. Rheological Properties of Peptide-Based Hydrogels for Biomedical and Other Applications. *Chem. Soc. Rev.* **2010**, *39*, 3528−3540.
(18) Parisi-Amon, A.; Mulyasasmita, W.; Chung, C.; Heilshorn, S. C. Protein-Engineered Injectable Hydrogel to Improve Retention of Transplanted Adipose-Derived Stem Cells. *Adv. Healthcare Mater.* **2013**, *2*, 428−432.
(19) Gaharwar, A. K.; Peppas, N. A.; Khademhosseini, A. Nanocomposite Hydrogels for Biomedical Applications. *Biotechnol. Bioeng.* **2014**, *111*, 441−453.
(20) Jaiswal, M. K.; Xavier, J. R.; Carrow, J. K.; Desai, P.; Alge, D.; Gaharwar, A. K. Mechanically Stiff Nanocomposite Hydrogels at Ultralow Nanoparticle Content. *ACS Nano* **2016**, *10*, 246−256.
(21) Utech, S.; Boccaccini, A. R. A Review of Hydrogel-Based Composites for Biomedical Applications: Enhancement of Hydrogel Properties by Addition of Rigid Inorganic Fillers. *J. Mater. Sci.* **2016**, *51*, 271−310.
(22) Costa, A. M. S.; Mano, J. F. Extremely Strong and Tough Hydrogels as Prospective Candidates for Tissue Repair − A Review. *Eur. Polym. J.* **2015**, *72*, 344−364.
(23) Dawson, J. I.; Oreffo, R. O. Clay: New Opportunities for Tissue Regeneration and Biomaterial Design. *Adv. Mater.* **2013**, *25*, 4069−4086.
(24) Wang, Q.; Mynar, J. L.; Yoshida, M.; Lee, E.; Lee, M.; Okuro, K.; Kinbara, K.; Aida, T. High-Water-Content Mouldable Hydrogels by Mixing Clay and a Dendritic Molecular Binder. *Nature* **2010**, *463*, 339−343.
(25) Wu, C.-J.; Gaharwar, A. K.; Schexnailder, P. J.; Schmidt, G. Development of Biomedical Polymer-Silicate Nanocomposites: A Materials Science Perspective. *Materials* **2010**, *3*, 2986.
(26) Yang, J.; Zhao, J.-J.; Xu, F.; Sun, R.-C. Revealing Strong Nanocomposite Hydrogels Reinforced by Cellulose Nanocrystals: Insight into Morphologies and Interactions. *ACS Appl. Mater. Interfaces* **2013**, *5*, 12960−12967.
(27) Okada, A.; Usuki, A. Twenty Years of Polymer-Clay Nanocomposites. *Macromol. Mater. Eng.* **2006**, *291*, 1449−1476.
(28) Yang, J.; Tighe, S. A Review of Advances of Nanotechnology in Asphalt Mixtures. *Procedia Soc. Behav. Sci.* **2013**, *96*, 1269−1276.
(29) Abdo, J.; Haneef, M. Clay Nanoparticles Modified Drilling Fluids for Drilling of Deep Hydrocarbon Wells. *Appl. Clay Sci.* **2013**, *86*, 76−82.
(30) Viseras, C.; Aguzzi, C.; Cerezo, P.; Lopez-Galindo, A. Uses of Clay Minerals in Semisolid Health Care and Therapeutic Products. *Appl. Clay Sci.* **2007**, *36*, 37−50.
(31) Li, M.-C.; Wu, Q.; Song, K.; Qing, Y.; Wu, Y. Cellulose Nanoparticles as Modifiers for Rheology and Fluid Loss in Bentonite Water-Based Fluids. *ACS Appl. Mater. Interfaces* **2015**, *7*, 5006−5016.
(32) de Sousa Rodrigues, L. A.; Figueiras, A.; Veiga, F.; de Freitas, R. M.; Nunes, L. C. C.; da Silva Filho, E. C.; da Silva Leite, C. M. The Systems Containing Clays and Clay Minerals from Modified Drug Release: A review. *Colloids Surf., B* **2013**, *103*, 642−651.
(33) Yu, Y.; Liu, Y.; Jia, F.; Li, S.; Kong, Y.; Zhang, E. Synthesis and Characterization of Temperature-Sensitive Poly (N-isopropylacrylamide-co-acrylamide)/Montmorillonite Nanocomposite Hydrogels. *Int. J. Polym. Mater.* **2013**, *62*, 34−38.
(34) Sirousazar, M.; Jahani-Javanmardi, A.; Kheiri, F.; Hassan, Z. M. *In Vitro* and *In Vivo* Assays on Egg White/Polyvinyl Alcohol/Clay Nanocomposite Hydrogel Wound Dressings. *J. Biomater. Sci., Polym. Ed.* **2016**, *27*, 1569−1583.
(35) Ghadiri, M.; Chrzanowski, W.; Lee, W. H.; Fathi, A.; Dehghani, F.; Rohanizadeh, R. Physico-Chemical, Mechanical and Cytotoxicity Characterizations of Laponite®/Alginate Nanocomposite. *Appl. Clay Sci.* **2013**, *85*, 64−73.
(36) Viseras, C.; Cerezo, P.; Sanchez, R.; Salcedo, I.; Aguzzi, C. Current Challenges in Clay Minerals for Drug Delivery. *Appl. Clay Sci.* **2010**, *48*, 291−295.
(37) Jin, Q.; Schexnailder, P.; Gaharwar, A. K.; Schmidt, G. Silicate Cross-Linked Bio-Nanocomposite Hydrogels from PEO and Chitosan. *Macromol. Biosci.* **2009**, *9*, 1028−1035.
(38) Takahashi, T.; Yamada, Y.; Kataoka, K.; Nagasaki, Y. Preparation of a Novel PEG−Clay Hybrid as a DDS Material: Dispersion Stability and Sustained Release Profiles. *J. Controlled Release* **2005**, *107*, 408−416.
(39) Song, F.; Li, X.; Wang, Q.; Liao, L.; Zhang, C. Nanocomposite Hydrogels and Their Applications in Drug Delivery and Tissue Engineering. *J. Biomed. Nanotechnol.* **2015**, *11*, 40−52.
(40) Oliva, N.; Shitreet, S.; Abraham, E.; Stanley, B.; Edelman, E. R.; Artzi, N. Natural Tissue Microenvironmental Conditions Modulate Adhesive Material Performance. *Langmuir* **2012**, *28*, 15402−15409.
(41) Conde, J.; Oliva, N.; Artzi, N. Implantable Hydrogel Embedded Dark-Gold Nanoswitch as a Theranostic Probe to Sense and Overcome Cancer Multidrug Resistance. *Proc. Natl. Acad. Sci. U. S. A.* **2015**, *112*, E1278−E1287.
(42) Conde, J.; Edelman, E. R.; Artzi, N. Target-Responsive DNA/RNA Nanomaterials for MicroRNA Sensing and Inhibition: The Jack-

DOI: 10.1021/acsnano.6b06730
ACS Nano 2017, 11, 2598−2610

of-All-Trades in Cancer Nanotheranostics? *Adv. Drug Delivery Rev.* **2015**, *81*, 169.
(43) Haraguchi, K.; Takehisa, T.; Fan, S. Effects of Clay Content on the Properties of Nanocomposite Hydrogels Composed of Poly(N-isopropylacrylamide) and Clay. *Macromolecules* **2002**, *35*, 10162−10171.
(44) Graphene Supermarket, carbon black; https://graphene-supermarket.com/Carbon-Black.html (accessed September 1, 2016).
(45) Sigma Product Specification, hydroxyapatite nanopowder <200 nm; http://www.sigmaaldrich.com/Graphics/COfAInfo/SigmaSAPQM/SPEC/67/677418/677418-BULK_____ALDRICH__.pdf (accessed September 1, 2016).
(46) Byk Technical Information, B-RI 21 Laponite performance additives; https://www.byk.com/fileadmin/byk/additives/product_groups/rheology/former_rockwood_additives/technical_brochures/BYK_B-RI21_LAPONITE_EN.pdf (accessed September 1, 2016).
(47) Rossi, S.; Luckham, P.; Tadros, T. F. Influence of Non-Ionic Polymers on the Rheological Behaviour of Na+-Montmorillonite Clay Suspensions—I Nonylphenol−Polypropylene Oxide−Polyethylene Oxide Copolymers. *Colloids Surf., A* **2002**, *201*, 85−100.
(48) Tamesue, S.; Ohtani, M.; Yamada, K.; Ishida, Y.; Spruell, J. M.; Lynd, N. A.; Hawker, C. J.; Aida, T. Linear versus Dendritic Molecular Binders for Hydrogel Network Formation with Clay Nanosheets: Studies with ABA Triblock Copolyethers Carrying Guanidinium Ion Pendants. *J. Am. Chem. Soc.* **2013**, *135*, 15650−15655.
(49) ten Brinke, A. J. W.; Bailey, L.; Lekkerkerker, H. N. W.; Maitland, G. C. Rheology Modification in Mixed Shape Colloidal Dispersions. Part II: Mixtures. *Soft Matter* **2008**, *4*, 337−348.
(50) Tawari, S. L.; Koch, D. L.; Cohen, C. Electrical Double-Layer Effects on the Brownian Diffusivity and Aggregation Rate of Laponite Clay Particles. *J. Colloid Interface Sci.* **2001**, *240*, 54−66.
(51) Neumann, B.; Sansom, K. The Formation of Stable Sols from Laponite, a Synthetic Hectorite-Like Clay. *Clay Miner.* **1970**, *8*, 389−404.
(52) Abend, S.; Lagaly, G. Sol−Gel Transitions of Sodium Montmorillonite Dispersions. *Appl. Clay Sci.* **2000**, *16*, 201−227.
(53) Ruzicka, B.; Zaccarelli, E. A Fresh Look at the Laponite Phase Diagram. *Soft Matter* **2011**, *7*, 1268−1286.
(54) Jabbari-Farouji, S.; Wegdam, G. H.; Bonn, D. Gels and Glasses in a Single System: Evidence for an Intricate Free-Energy Landscape of Glassy Materials. *Phys. Rev. Lett.* **2007**, *99*, 065701.
(55) Angelini, R.; Zaccarelli, E.; de Melo Marques, F. A.; Sztucki, M.; Fluerasu, A.; Ruocco, G.; Ruzicka, B. Glass−Glass Transition During Aging of a Colloidal Clay. *Nat. Commun.* **2014**, *5*, 4049.
(56) Bailey, L.; Lekkerkerker, H. N. W.; Maitland, G. C. Smectite Clay - Inorganic Nanoparticle Mixed Suspensions: Phase Behaviour and Rheology. *Soft Matter* **2015**, *11*, 222−236.
(57) Bailey, L.; Lekkerkerker, H. N. W.; Maitland, G. C. Rheology Modification of Montmorillonite Dispersions by Colloidal Silica. *Rheol. Acta* **2014**, *53*, 373−384.
(58) Ramsay, J. D. F.; Lindner, P. Small-Angle Neutron Scattering Investigations of the Structure of Thixotropic Dispersions of Smectite Clay Colloids. *J. Chem. Soc., Faraday Trans.* **1993**, *89*, 4207−4214.
(59) Michot, L. J.; Bihannic, I.; Porsch, K.; Maddi, S.; Baravian, C.; Mougel, J.; Levitz, P. Phase Diagrams of Wyoming Na-Montmorillonite Clay. Influence of Particle Anisotropy. *Langmuir* **2004**, *20*, 10829−10837.
(60) Paineau, E.; Michot, L. J.; Bihannic, I.; Baravian, C. Aqueous Suspensions of Natural Swelling Clay Minerals. 2. Rheological Characterization. *Langmuir* **2011**, *27*, 7806−7819.
(61) Xu, D.; Bhatnagar, D.; Gersappe, D.; Sokolov, J. C.; Rafailovich, M. H.; Lombardi, J. Rheology of Poly(N-isopropylacrylamide)−Clay Nanocomposite Hydrogels. *Macromolecules* **2015**, *48*, 840−846.
(62) Pujala, R. K.; Bohidar, H. B. Ergodicity Breaking and Aging Dynamics in Laponite-Montmorillonite Mixed Clay Dispersions. *Soft Matter* **2012**, *8*, 6120−6127.
(63) Joshi, N.; Rawat, K.; Aswal, V. K.; Bohidar, H. B. Smoluchowski Aggregation Kinetics, Gelation, Ergodicity Breaking and Aging Dynamics of (1:1) Laponite-Montmorillonite Mixed Clay Dispersions. *Colloids Surf., A* **2016**, *501*, 55−64.
(64) Pujala, R. K.; Pawar, N.; Bohidar, H. B. Universal Sol State Behavior and Gelation Kinetics in Mixed Clay Dispersions. *Langmuir* **2011**, *27* (9), 5193−5203.
(65) Rawat, K.; Agarwal, S.; Tyagi, A.; Verma, A. K.; Bohidar, H. B. Aspect Ratio Dependent Cytotoxicity and Antimicrobial Properties of Nanoclay. *Appl. Biochem. Biotechnol.* **2014**, *174*, 936−944.
(66) Pacelli, S.; Paolicelli, P.; Moretti, G.; Petralito, S.; Di Giacomo, S.; Vitalone, A.; Casadei, M. A. Gellan Gum Methacrylate and Laponite As an Innovative Nanocomposite Hydrogel for Biomedical Applications. *Eur. Polym. J.* **2016**, *77*, 114−123.
(67) Gaharwar, A. K.; Mihaila, S. M.; Swami, A.; Patel, A.; Sant, S.; Reis, R. L.; Marques, A. P.; Gomes, M. E.; Khademhosseini, A. Bioactive Silicate Nanoplatelets for Osteogenic Differentiation of Human Mesenchymal Stem Cells. *Adv. Mater.* **2013**, *25*, 3329−3336.
(68) Nones, J.; Riella, H. G.; Trentin, A. G.; Nones, J. Effects of Bentonite on Different Cell Types: A Brief Review. *Appl. Clay Sci.* **2015**, *105*−*106*, 225−230.
(69) Zhao, H.; Heindel, N. D. Determination of Degree of Substitution of Formyl Groups in Polyaldehyde Dextran by the Hydroxylamine Hydrochloride Method. *Pharm. Res.* **1991**, *8*, 400−402.
(70) Park, S.; Hung, C.; Ateshian, G. Mechanical Response of Bovine Articular Cartilage Under Dynamic Unconfined Compression Loading at Physiological Stress Levels. *Osteoarthr. Cartil.* **2004**, *12*, 65−73.

DOI: 10.1021/acsnano.6b06730
ACS Nano 2017, 11, 2598−2610